The Use of Huygens' Equivalence Principle for Solving 3D Volume Integral Equation of Scattering†

CAI-CHENG LU AND WENG CHO CHEW
DEPARTMENT OF ELECTRICAL AND COMPUTER ENGINEERING
UNIVERSITY OF ILLINOIS
URBANA, IL 61801

Abstract

A three dimensional (3D) version of the nested equivalent principle algorithm (NEPAL) is presented. In 3D, spherical wave functions are used to represent the scattered field of the subscatterers. Subscatterers are divided into different levels of groups in a nested manner. In other words, each group consists of two subgroups, and each subgroup contains two sub-subgroups, and so on. For each subgroup, the scattering solution is first solved and the number of subscatterers of the subgroup is then reduced by replacing the interior subscatterers with boundary subscatterers using Huygens' equivalence principle. As a result, when the subgroups are combined to form a higher level group, the group will have a smaller number of subscatterers. This process is repeated for each level, and in the last level, the number of subscatterers is proportional to that of boundary size of the subscatterers. This algorithm has a computational complexity of $O(N^2)$ in three dimensions and has the advantage of solving large scattering problems for multiple excitations. This is in contrast to Gaussian elimination which has a computational complexity of $O(N^3)$.

1. Introduction

The computation of electromagnetic scattering of three dimensional objects finds applications in many areas. Hence, it has been earnestly studied by many engineers, scientists and mathematicians alike. As a result, many algorithms have been developed for solving 3D scattering problems. Among these algorithms, finite difference time domain methods are popular due to their lower complexity and ease of implementations. However, many of these methods are for one excitation only, and the solution process needs to be repeated for multiple excitations. Moreover, absorbing boundary conditions are required for those algorithms. On the other hand, the solution to inte-

† This work was supported by Office of Naval Research under grant N00014-89-J1286, the Army Research Office under contract DAAL03-91-G-0339. The National Science Foundation under grant NSF ECS 92-24466, and NASA under grant NASA NAG 2-871. The computer time was provided by the National Center for Supercomputing Applications (NCSA) at the University of Illinois, Urbana-Champaign.

This paper will appear in IEEE AP Transaction.

File:nepal3d.tex, January 12, 1995

gral equations automatically satisfies the radiation condition. As a result, an integral equation solver with computational complexity comparable to differential equation solvers is a viable alternative solution technique to these scattering problems.

This paper presents an integral equation solver using the nested equivalence principle algorithm (NEPAL) which has been successfully applied to 2D problems [1]. It is known that in solving an integral equation, one can first replace the volume scatterer by small subscatterers where the size of a subscatterer is much smaller than a wavelength. The unknown function to be sought is expanded in terms of basis functions which usually have their supports on the subscatterers. By matching the field on the subscatterers, a set of linear equations are formed. The number of unknowns is proportional to the number of subscatterers in this case. Physically, each subscatterer can be considered a scattering center.

The interaction of a subscatterer with the other subscatterers can be described by interaction matrices [9]. If there are N subscatterers, then there will be N^2 interaction matrices since each subscatterer will interact with all the other subscatterers including itself. The N^2 interaction matrices can be found with N^3 operations [8,9]. The idea of NEPAL is to reduce the number of scattering centers, and hence to reduce the CPU time required for the solution, and essentially to find the inverse of the integral operator with computational complexity less than $O(N^3)$.

Similar algorithms for inversion of a matrix using nested dissection method for the finite element method can be found in [10]. It is shown in [1] that the computational complexity of NEPAL is asymptotically $N^{1.5}$ for 2D problems. In this paper, we will first formulate NEPAL for three dimensional problems and show that the complexity in 3D is N^2. In addition, we will use some of the symbols differently. For example, i is used either as a summation index or as the imaginary number $\sqrt{-1}$. The meaning is clear from the context.

2. Formulation of the Problem

A three dimensional volume can be discretized into a set of small cubic boxes called subscatterers. Each subscatterer has a volume Δ^3. The scattering property of each subscatterer can be represented by a multipole with order proportional to the electrical size of the subscatterer. The scattered field can be written as [2],

$$\begin{aligned}\mathbf{E}(\mathbf{r}) &= \sum_{nm} \left\{ \mathbf{M}_{nm}(\mathbf{r}-\mathbf{r}_i) \left[\mathbf{b}_i^M\right]_{nm} + \mathbf{N}_{nm}(\mathbf{r}-\mathbf{r}_i) \left[\mathbf{b}_i^E\right]_{nm} \right\} \\ &= \overline{\boldsymbol{\psi}}^t(\mathbf{r}-\mathbf{r}_i)\cdot\mathbf{b}_i, \end{aligned} \tag{1}$$

where, $\mathbf{b}_i = \left[\mathbf{b}_i^M, \mathbf{b}_i^E\right]^t$ is the multipole coefficients, superscripts M and E stand for TE and TM components respectively. Here, $\overline{\boldsymbol{\psi}}^t(\mathbf{r}) = [\mathbf{M}, \mathbf{N}]$ is the vector spherical wave function, and $\mathbf{M}$ and $\mathbf{N}$ are given by [2,4]

$$\mathbf{M}_{nm}(\mathbf{r}) = \hat{\theta}\frac{im}{\sin\theta} z_n(kr) Y_{nm}(\theta,\phi) - \hat{\phi} z_n(kr)\frac{\partial Y_{nm}(\theta,\phi)}{\partial\theta},$$

$$\begin{aligned}\mathbf{N}_{nm}(\mathbf{r}) =& \hat{r}\frac{n(n+1)}{kr} z_n(kr) Y_{nm}(\theta,\phi) + \hat{\theta}\frac{1}{kr}\frac{\partial}{\partial r}\left[r z_n(kr)\right]\frac{\partial Y_{nm}(\theta,\phi)}{\partial\theta} \\ &+ \hat{\phi}\frac{im}{kr\sin\theta}\frac{\partial}{\partial r}\left[r z_n(kr)\right] Y_{nm}(\theta,\phi).\end{aligned}$$

$$n = 1, 2, \cdots, \qquad m = -n, \cdots, n.$$

In the above, $z_n(kr)$ is a spherical Bessel function or spherical Hankel function of the first kind depending on whether $\overline{\boldsymbol{\psi}}^t(\mathbf{r})$ is an incoming wave or an outgoing wave, respectively. When Bessel function is used, $\Re g\overline{\boldsymbol{\psi}}$, means the regular part of $\overline{\boldsymbol{\psi}}$, which replaces $\overline{\boldsymbol{\psi}}$. In the above, Y_{nm} is a spherical harmonic, and it is defined by [4]

$$Y_{nm}(\theta,\phi) = (-1)^m\sqrt{\frac{2n+1}{4\pi}\frac{(n-m)!}{(n+m)!}} P_n^m(\cos\theta) e^{im\phi}, \qquad m \geq 0,$$

$$Y_{nm}(\theta,\phi) = (-1)^{|m|} Y_{n|m|}(\theta,\phi), \qquad m < 0,$$

where, P_n^m is the associated Legendre function.

Expressing the incident field in the same manner,

$$\mathbf{E}^{inc}(\mathbf{r}) = \Re g\overline{\boldsymbol{\psi}}^t(\mathbf{r}-\mathbf{r}_i)\cdot\overline{\boldsymbol{\alpha}}_{is}\cdot\mathbf{a}_s, \tag{2}$$

we can relate the unknown coefficient $\mathbf{b}_i$ to $\mathbf{a}_s$ via a T-matrix by matching the field on the boundary of the subscatterer [2,6,7]:

$$\mathbf{b}_i = \overline{\mathbf{T}} \cdot \overline{\boldsymbol{\alpha}}_{is} \cdot \mathbf{a}_s. \tag{3}$$

In the above, $\overline{\boldsymbol{\alpha}}_{is}$ is a translation matrix [2,5] that changes the coordinates of the multipole expansions, and $\mathbf{a}_s$ is the incident wave amplitude.

When Δ is small, the T-matrix is diagonal and can be approximated by that of an equivolume sphere,* and can be found using the Mie series [2]. When N_A subscatterers are present, the coefficients $\mathbf{b}_i$ will be unknown which satisfy the following brute force equations [7,12,13]:

$$\mathbf{b}_i = \overline{\mathbf{T}}_i \cdot \left[\overline{\boldsymbol{\alpha}}_{is} \cdot \mathbf{a}_s + \sum_{\substack{j=1 \\ j \neq i}}^{N_A} \overline{\boldsymbol{\alpha}}_{ij} \cdot \mathbf{b}_j \right], \qquad i = 1, 2, \cdots, N_A. \tag{4}$$

Since the solution to the above equations has to be linearly proportional to $\overline{\boldsymbol{\alpha}}_{js} \cdot \mathbf{a}_s$, it can be written as

$$\mathbf{b}_i = \sum_{j=1}^{N_A} \overline{\mathbf{I}}_{ij(N_A)} \cdot \overline{\boldsymbol{\alpha}}_{js} \cdot \mathbf{a}_s, \qquad i = 1, 2, \cdots, N_A. \tag{5}$$

Hence, the scattered field is given by

$$\mathbf{E}^{sca}(\mathbf{r}) = \sum_{i=1}^{N_A} \overline{\boldsymbol{\psi}}^t(\mathbf{r} - \mathbf{r}_i) \cdot \sum_{j=1}^{N_A} \overline{\mathbf{I}}_{ij(N_A)} \cdot \overline{\boldsymbol{\alpha}}_{js} \cdot \mathbf{a}_s. \tag{6}$$

In the above, $\overline{\mathbf{I}}_{ij(N_A)}$, $i, j = 1, 2, \cdots, N_A$ are called interaction matrices; they describe the interactions between N_A subscatterers. They also describe a scattering process whereby the wave enters through the j-th scattering center, and leaves through the i-th scattering center. They can be found in a variety of ways, for example, by Gaussian elimination, or by a recursive algorithm [8,9].

3. Equivalence of Interaction Matrices.

As shown in the above section, the scattered field can be determined by the N_A^2 interaction matrices for a group of N_A subscatterers. In this section,

* This approximation was first used by Richmond [11].

Definition : Two sets of interaction matrices $\overline{\mathbf{I}}_{ij(N_A)}$ and $\overline{\mathbf{I}}_{ij(N_B)}$ are said to be equivalent if they generate the same scattered field via Equation (6) for the same incident field.

we will show by the Huygens' equivalence principle that there is another set of interaction matrices which will generate the same scattered field. To this end, we first give a definition of equivalent interaction matrices.

In the following, we will give a mathematical description for the equivalence of the interior subscatterers by those on the surface using Huygens' equivalence principle [3] (see Figure 1).

First, we assume that S is the boundary of a volume region V, and V contains sources which generate field $\mathbf{E}$ and $\mathbf{H}$ on the boundary. Next, we let $\mathbf{r}'$ be a point outside V, as shown in Figure 2. Huygens' equivalence principle states that the field at $\mathbf{r}'$ due to sources inside V can be represented via equivalent sources on the boundary:

$$\mathbf{E}(\mathbf{r}') = -\oint_S dS \left[\hat{n} \times \mathbf{E}(\mathbf{r}) \cdot \nabla \times \overline{\mathbf{G}}_e(\mathbf{r}, \mathbf{r}') + i\omega\mu\hat{n} \times \mathbf{H}(\mathbf{r}) \cdot \overline{\mathbf{G}}_e(\mathbf{r}, \mathbf{r}')\right], \quad (7)$$

where,

$$\overline{\mathbf{G}}_e(\mathbf{r}, \mathbf{r}') = \left(\overline{\mathbf{I}} + \frac{\nabla\nabla}{k^2}\right) \frac{e^{ik|\mathbf{r}-\mathbf{r}'|}}{4\pi|\mathbf{r}-\mathbf{r}'|} \quad (7a)$$

is the free space dyadic Green's function. Equation (7) has a double roles. First, it provides an indirect approach to compute the field at points outside V. Second, it tells us how to construct the equivalent sources: the equivalent sources are simply the tangential components of the fields, which are electric and magnetic surface currents.

Apart from the above two points, we also observed that: (1) The equivalence principle does not specify the type and the number of the original sources inside V; they could be any kind of sources: induced sources, other equivalent sources, a point source, several point sources or distributed sources. (2) The equivalent sources are uniquely determined by the shape of the surface and the density of the tangential field components. This allows us to replace a large number of sources with a relatively small number of sources.

The mathematical representation of a source can be different. For example, Equation (2) represents an incident field represented by its multipole expansion about the source point, while Equation (6) represents the induced sources by a set of matrices $\overline{\mathbf{I}}_{ij(N_A)}$, $i,j = 1,2,\cdots,N_A$. Similarly, we can represent equivalent sources in the same manner, i.e., via another set of interaction matrices $\overline{\mathbf{I}}_{ij(N_B)}, i,j = 1,2,\cdots,N_B$. We shall now construct the relation between the two sets of matrices using Equation (7).

First, we divide the surface S into N_B small surfaces or patches, where each patch is of area ΔS. As a result, Equation (7) can be replaced by a discrete summation yielding

$$\mathbf{E}(\mathbf{r}') = -\sum_{i=1}^{N_B} \Delta S \left[\hat{n} \times \mathbf{E}(\mathbf{r}_i) \cdot \nabla \times \overline{\mathbf{G}}_e(\mathbf{r}_i, \mathbf{r}') + i\omega\mu\hat{n} \times \mathbf{H}(\mathbf{r}_i) \cdot \overline{\mathbf{G}}_e(\mathbf{r}_i, \mathbf{r}')\right]. \tag{8}$$

At the i-th patch, we let $\mathbf{r} = \mathbf{r}'' + \mathbf{r}_i$. Here, $\mathbf{r}''$ is the local coordinate for the i-th patch. Then,

$$\mathbf{r} - \mathbf{r}' = \mathbf{r}'' + \mathbf{r}_i - \mathbf{r}' = \mathbf{r}'' - (\mathbf{r}' - \mathbf{r}_i). \tag{9}$$

Under the condition that $|\mathbf{r}' - \mathbf{r}_i| > |\mathbf{r}''|$, the Green's function $\overline{\mathbf{G}}_e(\mathbf{r}, \mathbf{r}')$ can be expanded as ($\mathbf{r}'_i = \mathbf{r}' - \mathbf{r}_i$, [3, p.409])

$$\overline{\mathbf{G}}_e(\mathbf{r}'', \mathbf{r}'_i) = \sum_{nm} \frac{ik(-)^m}{n(n+1)} \left[\Re g\mathbf{M}_{n,-m}(\mathbf{r}'')\mathbf{M}_{nm}(\mathbf{r}'_i) + \Re g\mathbf{N}_{n,-m}(\mathbf{r}'')\mathbf{N}_{nm}(\mathbf{r}'_i)\right]. \tag{10}$$

Then it is easy to show that

$$\overline{\mathbf{G}}_e(\mathbf{r}_i, \mathbf{r}') = \overline{\mathbf{G}}_e(\mathbf{r}'' = 0, \mathbf{r}'_i). \tag{11}$$

Consequently, Equation (8) can be written more compactly as

$$\mathbf{E}(\mathbf{r}') = \sum_i \sum_{nm} \left\{\mathbf{M}_{nm}(\mathbf{r}'_i) \cdot [\mathbf{b}_i^M]_{nm} + \mathbf{N}_{nm}(\mathbf{r}'_i) \cdot [\mathbf{b}_i^E]_{nm}\right\}, \tag{12}$$

where

$$[\mathbf{b}_i^M]_{nm} = \frac{-ik^2(-)^m}{n(n+1)} \Delta S\Big[\hat{n}_i \times \mathbf{E}(\mathbf{r}_i) \cdot \Re g\mathbf{N}_{n,-m}(0)\Big], \tag{13a}$$

$$[\mathbf{b}_i^E]_{nm} = \frac{-ik^2(-)^m}{n(n+1)} \Delta S\Big[i\eta\hat{n}_i \times \mathbf{H}(\mathbf{r}_i) \cdot \Re g\mathbf{N}_{n,-m}(0)\Big], \tag{13b}$$

$\hat{n}_i$ is the average normal of the i-th patch, and $\eta = \sqrt{\mu_0/\epsilon_0}$ is the free space impedance.

In the above derivation, the identities

$$\nabla \times \mathbf{M} = k\mathbf{N}, \qquad \nabla \times \mathbf{N} = k\mathbf{M}$$

have been used. Equation (12) gives the source-field relation for the equivalent sources on the surface S.

We assume that the source-field relation for the interior sources is of the form as Equation (1) with multipole amplitude given by $\mathbf{a}_j$, $j = 1, 2, ..., N_A$. Then,

$$\mathbf{E}(\mathbf{r}) = \sum_{j,\nu\mu} \Big\{ \mathbf{M}_{\nu\mu}(\mathbf{r} - \mathbf{r}_j) \cdot [\mathbf{a}_j^M]_{\nu\mu} + \mathbf{N}_{\nu\mu}(\mathbf{r} - \mathbf{r}_j) \cdot [\mathbf{a}_j^E]_{\nu\mu} \Big\}, \tag{14a}$$

$$\mathbf{H}(\mathbf{r}) = \frac{1}{i\eta} \sum_{j,\nu\mu} \Big\{ \mathbf{N}_{\nu\mu}(\mathbf{r} - \mathbf{r}_j) \cdot [\mathbf{a}_j^M]_{\nu\mu} + \mathbf{M}_{\nu\mu}(\mathbf{r} - \mathbf{r}_j) \cdot [\mathbf{a}_j^E]_{\nu\mu} \Big\}. \tag{14b}$$

We let $\mathbf{r} = \mathbf{r}_i$ in Equations (14a) and (14b), and substitute them into Equation (13a), we have

$$\begin{aligned}[\mathbf{b}_i^M]_{nm} =& \frac{-ik^2(-)^m}{n(n+1)} \Delta S \Re g \mathbf{N}_{n,-m}(0) \\ & \cdot \sum_{j,\nu\mu} \Big(\hat{n}_i \times \mathbf{M}_{\nu\mu}(\mathbf{r}_{ji}) \cdot [\mathbf{a}_j^M]_{\nu\mu} + \hat{n}_i \times \mathbf{N}_{\nu\mu}(\mathbf{r}_{ji}) \cdot [\mathbf{a}_j^E]_{\nu\mu} \Big),\end{aligned}$$

where, $\mathbf{r}_{ji} = \mathbf{r}_i - \mathbf{r}_j$. Alternatively, we can write the above as

$$[\mathbf{b}_i^M]_{nm} = \sum_{j,\nu\mu} \left\{ [\overline{\mathbf{c}}_{ij}^{MM}]_{nm,\nu\mu} \cdot [\mathbf{a}_j^M]_{\nu\mu} + [\overline{\mathbf{c}}_{ij}^{ME}]_{nm,\nu\mu} \cdot [\mathbf{a}_j^E]_{\nu\mu} \right\}. \tag{15a}$$

Similarly, we have

$$[\mathbf{b}_i^E]_{nm} = \sum_{j,\nu\mu} \left\{ [\overline{\mathbf{c}}_{ij}^{EM}]_{nm,\nu\mu} \cdot [\mathbf{a}_j^M]_{\nu\mu} + [\overline{\mathbf{c}}_{ij}^{EE}]_{nm,\nu\mu} \cdot [\mathbf{a}_j^E]_{\nu\mu} \right\}. \tag{15b}$$

In the above,

$$[\overline{\mathbf{c}}_{ij}^{MM}]_{nm,\nu\mu} = \frac{-ik^2(-)^m}{n(n+1)} \Delta S \Re g \mathbf{N}_{n,-m}(0) \cdot \hat{n}_i \times \mathbf{M}_{\nu\mu}(\mathbf{r}_{ji}), \tag{16a}$$

$$[\overline{\mathbf{c}}_{ij}^{ME}]_{nm,\nu\mu} = \frac{-ik^2(-)^m}{n(n+1)} \Delta S \Re g \mathbf{N}_{n,-m}(0) \cdot \hat{n}_i \times \mathbf{N}_{\nu\mu}(\mathbf{r}_{ji}), \tag{16b}$$

$$[\overline{\mathbf{c}}_{ij}^{EM}]_{nm,\nu\mu} = [\overline{\mathbf{c}}_{ij}^{ME}]_{nm,\nu\mu}, \tag{16c}$$

$$[\overline{\mathbf{c}}_{ij}^{EE}]_{nm,\nu\mu} = [\overline{\mathbf{c}}_{ij}^{MM}]_{nm,\nu\mu}. \tag{16d}$$

Denoting

$$\overline{\mathbf{h}}_{ij}^{(o)} = \overline{\mathbf{c}}_{ij} = \begin{bmatrix} \overline{\mathbf{c}}_{ij}^{MM} & \overline{\mathbf{c}}_{ij}^{ME} \\ \overline{\mathbf{c}}_{ij}^{EM} & \overline{\mathbf{c}}_{ij}^{EE} \end{bmatrix},$$

we have the relation between the equivalent sources and the original sources:

$$\mathbf{b}_i = \sum_j \overline{\mathbf{h}}_{ij}^{(o)} \cdot \mathbf{a}_j,$$

where $\mathbf{b}_i = [\mathbf{b}_i^M, \mathbf{b}_i^E]^t$ and $\mathbf{a}_j = [\mathbf{a}_j^M, \mathbf{a}_j^E]^t$. If there is only one interior source located at $\mathbf{r}_j$ inside V, then the field at $\mathbf{r}'$ corresponding to this source is given by (14a) with $N_A = 1$, or

$$\mathbf{E}(\mathbf{r}') = \overline{\boldsymbol{\psi}}^t(\mathbf{r}' - \mathbf{r}_j) \cdot \mathbf{a}_j.$$

The above is the direct source-field relation. On the other hand, we have an indirect source-field relation in Equation (12) via the Huygens' equivalence principle, or

$$\mathbf{E}(\mathbf{r}') = \sum_{i=1}^{N_B} \overline{\boldsymbol{\psi}}^t(\mathbf{r}' - \mathbf{r}_i) \cdot \overline{\mathbf{h}}_{ij}^{(o)} \cdot \mathbf{a}_j.$$

Equating the two representations, we have for an arbitrary $\mathbf{a}_j$,

$$\overline{\boldsymbol{\psi}}^t(\mathbf{r} - \mathbf{r}_j) = \sum_{i=1}^{N_B} \overline{\boldsymbol{\psi}}^t(\mathbf{r} - \mathbf{r}_i) \cdot \overline{\mathbf{h}}_{ij}^{(o)}. \tag{17}$$

Equation (17) is the first equation which will be used to derive the equivalence between interaction matrices of interior subscatterers and boundary subscatterers.

Now we consider the reverse problem: the sources are outside of V and we need to compute the field at $\mathbf{r}'$ inside V due to outside sources. Using similar steps as in deriving $\overline{\mathbf{h}}_{ii'}^{(o)}$, we can write the field $\mathbf{E}(\mathbf{r}')$ in the same form as Equations (12), (13a) and (13b), except that $\mathbf{r}'$ is insider V in this case.

Suppose that the source is located at $\mathbf{r}_s$ with the multipole amplitude $\mathbf{a}_s$, then the fields at $\mathbf{r}$ due to this source are given by

$$\mathbf{E}(\mathbf{r}) = \sum_{\nu\mu} \Big\{ \mathbf{M}_{\nu\mu}(\mathbf{r}-\mathbf{r}_s) \cdot [\mathbf{a}_s^M]_{\nu\mu} + \mathbf{N}_{\nu\mu}(\mathbf{r}-\mathbf{r}_s) \cdot [\mathbf{a}_s^E]_{\nu\mu} \Big\}, \tag{18a}$$

$$\mathbf{H}(\mathbf{r}) = \frac{1}{i\eta} \sum_{\nu\mu} \Big\{ \mathbf{N}_{\nu\mu}(\mathbf{r}-\mathbf{r}_s) \cdot [\mathbf{a}_s^M]_{\nu\mu} + \mathbf{M}_{\nu\mu}(\mathbf{r}-\mathbf{r}_s) \cdot [\mathbf{a}_s^E]_{\nu\mu} \Big\}. \tag{18b}$$

Equation (18) gives an outgoing wave centered at $\mathbf{r}_s$, and the field point $\mathbf{r}$ is not specified yet. Now, we let $\mathbf{r}$ be a point in the vicinity of $\mathbf{r}_i \in S$, with $i = 1, 2, ..., N_B$. Observe that at $\mathbf{r}$, the field can also be considered incoming waves centered at $\mathbf{r}_i$. This is more rigorously given by the vector wave translation equation from the vector addition theorem [4,5]:

$$\mathbf{M}(\mathbf{r}-\mathbf{r}_s) = \Re g\mathbf{M}(\mathbf{r}-\mathbf{r}_i) \cdot \overline{\mathbf{A}}_{is} + \Re g\mathbf{N}(\mathbf{r}-\mathbf{r}_i) \cdot \overline{\mathbf{B}}_{is},$$
$$\mathbf{N}(\mathbf{r}-\mathbf{r}_s) = \Re g\mathbf{M}(\mathbf{r}-\mathbf{r}_i) \cdot \overline{\mathbf{B}}_{is} + \Re g\mathbf{N}(\mathbf{r}-\mathbf{r}_i) \cdot \overline{\mathbf{A}}_{is}.$$

Therefore, the above can be rewritten as

$$\mathbf{E}(\mathbf{r}) = \sum_{\nu\mu} \Big\{ \Re g\mathbf{M}_{\nu\mu}(\mathbf{r}-\mathbf{r}_i) \cdot [\mathbf{a}_{is}^M]_{\nu\mu} + \Re g\mathbf{N}_{\nu\mu}(\mathbf{r}-\mathbf{r}_i) \cdot [\mathbf{a}_{is}^E]_{\nu\mu} \Big\}, \tag{18c}$$

$$\mathbf{H}(\mathbf{r}) = \frac{1}{i\eta} \sum_{\nu\mu} \Big\{ \Re g\mathbf{N}_{\nu\mu}(\mathbf{r}-\mathbf{r}_i) \cdot [\mathbf{a}_{is}^M]_{\nu\mu} + \Re g\mathbf{M}_{\nu\mu}(\mathbf{r}-\mathbf{r}_i) \cdot [\mathbf{a}_{is}^E]_{\nu\mu} \Big\}, \tag{18d}$$

where, $\mathbf{a}_{is}$ is related to $\mathbf{a}_s$ by

$$\mathbf{a}_{is} = \begin{bmatrix} \overline{\mathbf{A}}_{is} & \overline{\mathbf{B}}_{is} \\ \overline{\mathbf{B}}_{is} & \overline{\mathbf{A}}_{is} \end{bmatrix} \cdot \mathbf{a}_s = \overline{\boldsymbol{\alpha}}_{is} \cdot \mathbf{a}_s.$$

Substitution of (18c) and (18d) into Equation (13a), we have

$$[\mathbf{b}_i^M]_{nm} = \frac{-ik^2(-)^m}{n(n+1)} \Delta S \Re g\mathbf{N}_{n,-m}(0)$$
$$\cdot \hat{n}_i \times \sum_{\nu\mu} \Big(\Re g\mathbf{M}_{\nu\mu}(0) \cdot [\mathbf{a}_{is}^M]_{\nu\mu} + \Re g\mathbf{N}_{\nu\mu}(0) \cdot [\mathbf{a}_{is}^E]_{\nu\mu} \Big),$$

or

$$[\mathbf{b}_i^M]_{nm} = \sum_{\nu\mu} \left\{ [\mathbf{c}_i^{MM}]_{nm,\nu\mu} \cdot [\mathbf{a}_{is}^M]_{\nu\mu} + [\mathbf{c}_i^{ME}]_{nm,\nu\mu} \cdot [\mathbf{a}_{is}^E]_{\nu\mu} \right\}. \tag{19a}$$

Similarly, we have

$$[\mathbf{b}_i^E]_{nm} = \sum_{\nu\mu} \left\{ [\mathbf{c}_i^{EM}]_{nm,\nu\mu} \cdot [\mathbf{a}_{is}^M]_{\nu\mu} + [\mathbf{c}_i^{EE}]_{nm,\nu\mu} \cdot [\mathbf{a}_{is}^E]_{\nu\mu} \right\}. \tag{19b}$$

Hence,

$$\mathbf{b}_i = \overline{\mathbf{c}}_i \cdot \mathbf{a}_s = \begin{bmatrix} \overline{\mathbf{c}}_i^{MM} & \overline{\mathbf{c}}_i^{ME} \\ \overline{\mathbf{c}}_i^{ME} & \overline{\mathbf{c}}_i^{EE} \end{bmatrix} \cdot \mathbf{a}_{is}, \tag{19c}$$

where,

$$[\mathbf{c}_i^{MM}]_{nm,\nu\mu} = \frac{-ik^2(-)^m}{n(n+1)} \Delta S \Re g \mathbf{N}_{n,-m}(0) \cdot \hat{n}_i \times \Re g \mathbf{M}_{\nu\mu}(0), \tag{20a}$$

$$[\mathbf{c}_i^{ME}]_{nm,\nu\mu} = \frac{-ik^2(-)^m}{n(n+1)} \Delta S \Re g \mathbf{N}_{n,-m}(0) \cdot \hat{n}_i \times \Re g \mathbf{N}_{\nu\mu}(0), \tag{20b}$$

$$[\mathbf{c}_i^{EM}]_{nm,\nu\mu} = [\mathbf{c}_i^{ME}]_{nm,\nu\mu}, \tag{20c}$$

$$[\mathbf{c}_i^{EE}]_{nm,\nu\mu} = [\mathbf{c}_i^{MM}]_{nm,\nu\mu}. \tag{20d}$$

In the above,

$$\Re g \mathbf{M}_{\nu\mu}(0) = 0,$$

and

$$\Re g \mathbf{N}_{\nu\mu}(0) = 0, \qquad \nu \neq 1,$$

$$\Re g \mathbf{N}_{1,\mp 1}(0) = \frac{2}{3}\sqrt{\frac{3}{8\pi}}(\pm\hat{x} - i\hat{y}),$$
$$\Re g \mathbf{N}_{1,0}(0) = \frac{2}{3}\sqrt{\frac{3}{4\pi}}\hat{z}.$$

Now, assume that the source is located outside V at $\mathbf{r}_s$, and $\mathbf{r}_j$ is an interior point, the incident field in the vicinity of $\mathbf{r}_j$ due to source at $\mathbf{r}_s$ can be written as

$$\mathbf{E}^{inc}(\mathbf{r}) = \Re g \overline{\boldsymbol{\psi}}^t(\mathbf{r} - \mathbf{r}_j) \cdot \overline{\boldsymbol{\alpha}}_{js} \cdot \mathbf{a}_s. \tag{21}$$

Applying the equivalence principle, this field can be thought of as coming from the equivalent sources on the boundary:

$$\mathbf{E}^{inc}(\mathbf{r}) = \sum_{i=1}^{N_B} \overline{\boldsymbol{\psi}}^t(\mathbf{r} - \mathbf{r}_i) \cdot \mathbf{b}_i, \tag{22}$$

where $\mathbf{b}_i$ is given by (19c).

Using translation formula to translate $\overline{\boldsymbol{\psi}}^t(\mathbf{r} - \mathbf{r}_i)$, the outgoing wave originated at $\mathbf{r}_i$, to an incoming wave centered at $\mathbf{r}_j$, we have,

$$\overline{\boldsymbol{\psi}}^t(\mathbf{r} - \mathbf{r}_i) = \Re g \overline{\boldsymbol{\psi}}^t(\mathbf{r} - \mathbf{r}_j) \cdot \overline{\boldsymbol{\alpha}}_{ji}. \tag{23}$$

Substituting $\overline{\boldsymbol{\psi}}^t(\mathbf{r}-\mathbf{r}_i)$ in (21) by (23), and equating the resultant equation and (22) for arbitrary point $\mathbf{r}$ near $\mathbf{r}_j$, we obtain:

$$\overline{\boldsymbol{\alpha}}_{js}\cdot\mathbf{a}_s=\sum_{i=1}^{N_B}\overline{\boldsymbol{\alpha}}_{ji}\cdot\overline{\mathbf{c}}_i\cdot\overline{\boldsymbol{\alpha}}_{is}\cdot\mathbf{a}_s=\sum_{i=1}^{N_B}\overline{\mathbf{h}}_{ji}^{(i)}\cdot\overline{\boldsymbol{\alpha}}_{is}\cdot\mathbf{a}_s, \tag{24}$$

with

$$\overline{\mathbf{h}}_{ji}^{(i)}=\overline{\boldsymbol{\alpha}}_{ji}\cdot\overline{\mathbf{c}}_i. \tag{25}$$

Equation (24) is the second equation which will be used for our equivalence problem.

With Equations (17) and (24), we can easily relate the equivalent interaction matrices $\overline{\mathbf{I}}_{ij(N_B)}$ with the original ones $\overline{\mathbf{I}}_{ij(N_A)}$. To this end, we start with Equation (6), and replace $\overline{\boldsymbol{\psi}}^t(\mathbf{r}-\mathbf{r}_i)$ in it by Equation (17), and replace $\overline{\boldsymbol{\alpha}}_{is}\cdot\mathbf{a}_s$ by Equation (24), to obtain

$$\mathbf{E}^{sca}(\mathbf{r})=\sum_{m=1}^{N_B}\overline{\boldsymbol{\psi}}^t(\mathbf{r}-\mathbf{r}_m)\cdot\sum_{i=1}^{N_A}\overline{\mathbf{h}}_{mi}^{(o)}\cdot\sum_{j=1}^{N_A}\overline{\mathbf{I}}_{ij(N_A)}\cdot\sum_{m'=1}^{N_B}\overline{\mathbf{h}}_{jm'}^{(i)}\cdot\overline{\boldsymbol{\alpha}}_{m's}\cdot\mathbf{a}_s. \tag{26}$$

The above can be rewritten as

$$\mathbf{E}^{sca}(\mathbf{r})=\sum_{m=1}^{N_B}\overline{\boldsymbol{\psi}}^t(\mathbf{r}-\mathbf{r}_m)\cdot\sum_{m'=1}^{N_B}\overline{\mathbf{I}}_{mm'(N_B)}\cdot\overline{\boldsymbol{\alpha}}_{m's}\cdot\mathbf{a}_s, \tag{27}$$

where

$$\overline{\mathbf{I}}_{mm'(N_B)}=\sum_{i=1}^{N_A}\overline{\mathbf{h}}_{mi}^{(o)}\cdot\sum_{j=1}^{N_A}\overline{\mathbf{I}}_{ij(N_A)}\cdot\overline{\mathbf{h}}_{jm'}^{(i)}. \tag{28}$$

Equation (28) specifies the equivalence relation between the original interaction matrices and the equivalent ones. This is the key equation for NEPAL. We will explain how this equation is used to reduce the number of interaction matrices.

For a volume scatterer, the total subscatterers are divided into boundary subscatterers and interior subscatterers. If we define $\overline{\mathbf{h}}_{mi}^{(o)}=\overline{\mathbf{h}}_{mi}^{(i)}=\overline{\mathbf{I}}$ for $i=m$, then the right hand side of Equation (28) may also include interaction matrices of boundary subscatterers. Let N_A be the total number of subscatterers, and N_B, the number of boundary subscatterers. Then the number of interaction matrices is reduced from N_A^2 to N_B^2. This could be significant if $N_B \ll N_A$ as shown in Figure 1. Furthermore, there is no violation of addition theorem in using this equivalence principle.

4. The Nested Equivalence Principle Algorithm (NEPAL)

As mentioned in the introduction of this paper, the idea of NEPAL is to reduce the number of scattering centers, or the number of interaction matrices, as shown by Equation (28). In this section, we will describe the steps involved in this algorithm .

To begin, the subscatterers are first divided into different levels of groups in a nested manner, i.e., a group of one level is divided into two subgroups of the next lower level. Each subgroup is again divided into two sub-subgroups of one level lower than that of the subgroup, and so on. The process continues until the lowermost level of subgroups which contains 64 subscatterers is reached as shown in Figure 3, where each of the cubes shown contains 64 subscatterers. In each level, we find the scattering solution for each of the subgroups, and then use Huygens' equivalence principle (Equation (28)) to replace the interior subscatterers of a subgroup by subscatterers on the boundary. For example, in the lowermost level, we first solve for the scattering solution for each subgroup of 64 subscatterers. Then Equation (28) is used to remove the interior subscatterers. In this level, there are only eight interior subscatterers for each subgroup. After this step, each subgroup contains 56 subscatterers with known solution.

Next we go to the next higher level—the second level. In this level, each subgroup contains 112 subscatterers, as it is made up of two subgroups of 56 subscatterers.* The solution to the 112 subscatterers together is not known. Hence, we first solve for the scattering solution for each subgroup with 112 subscatterers. Then their interior subscatterers (8 for each subgroup in this level) are removed via Equation (28) and 104 subscatterers remain in each subgroup with known solution.

We can see that at each level, upon removal of the interior subscatterers,

* Alternatively, one can proceed to the next level by groups of 4 or groups of 8, but we have found that groups of 2 to be most expedient.

a subgroup contains less subscatterers than what it originally contained. The process is continued until the highest level is reached, where there is only one group which is made up of two lower level subgroups. Again, the solution must be sought for the group. However, since interior subscatterers for the two subgroups are removed, this group contains much less subscatterers than N_A if N_A is the total number of subscatterers for the original problem. As a result, much less operations are expended to find the final solution.

It is seen that the operation at each level contains two parts: one to find the scattering solution, the other to remove the interior subscatterers. It is important that the removal of the interior subscatterers of a group does not change the scattering property of the subgroup. The solution of interaction matrices can be found in the same way as described in [1].

Using similar analysis as presented for the 2D case, the computational complexity can be shown to be CN^2 for N spheres, where C is roughly 900.

5. Parallelization of the Code on CM-5

The Connection Machine CM-5 of Thinking Machine Corp. at the National Center for Supercomputing Application at the University of Illinois is a massively parallel processor (MPP) machine with 512 processors. A version of NEPAL was first written on a SUN SPARC workstation which was a serial machine. The version of the code did not run efficiently on a massively parallel machine. Much of the code has to be rewritten for an MPP machine.

There are two major processes in implementing NEPAL: they are the interaction matrix algorithm (IMA) process and the equivalence principle process. The IMA consumed most of the CPU time. When NEPAL was first implemented on the CM-5, the code called an external function in the library of CM-5. This function inverted a matrix by Gauss-Jordan method (the name of the function was "gen_gj_invert"). When this function was called in the IMA part, the CPU time for matrix fill was dominant, because the matrix inverse was greatly expedited. This was not the case on a serial machine. Hence, the matrix fill had to be expedited as follows.

The matrix involved in the IMA can be written as

$$\overline{\mathbf{A}} = [\overline{\mathbf{A}}_{ij}] \tag{29}$$

where $\overline{\mathbf{A}}_{ij}$ are block matrices.

$$\overline{\mathbf{A}}_{ij} = \begin{cases} \overline{\mathbf{I}}, & i = j, \\ -\overline{\mathbf{T}}_{k(1)} \cdot \overline{\boldsymbol{\alpha}}_{ij}, & i \pm j, \end{cases} \tag{30}$$

and $\overline{\mathbf{T}}_{i(1)}$ are the isolated T-matrix. $\overline{\boldsymbol{\alpha}}_{ij}$ are the wave translation matrices[2]. For this specific problem, the size of the subscatterer is small compared to wavelength. As a result, the size of the translation matrices is 6×6, as it can be given explicitly as:

$$\overline{\mathbf{A}}_{ij} = \begin{bmatrix} \overline{\boldsymbol{\alpha}} & \overline{\boldsymbol{\beta}} \\ \overline{\boldsymbol{\beta}} & \overline{\boldsymbol{\alpha}} \end{bmatrix} \tag{31}$$

where

$$\begin{aligned}
[\overline{\boldsymbol{\alpha}}_{ij}]_{12} &= \frac{3}{2\sqrt{2}} h_2 \sin\theta_{ij} \cos\theta_{ij} e^{i\phi_{ij}} \\
[\overline{\boldsymbol{\alpha}}_{ij}]_{22} &= h_0 + h_2(1.5\cos^2\theta_{ij} - \frac{1}{2}) \\
[\overline{\boldsymbol{\alpha}}_{ij}]_{13} &= -0.75 \sin^2\theta_{ij} h_2 e^{i2\phi_{ij}} \\
[\overline{\boldsymbol{\alpha}}_{ij}]_{33} &= h_0 - \frac{1}{2}([\alpha_{ij}]_{22} - h_0) \\
[\overline{\boldsymbol{\beta}}_{ij}]_{12} &= \frac{3i}{2\sqrt{2}} h_1 \sin\theta_{ij} e^{i\phi_{ij}}
\end{aligned}$$

$$\begin{aligned}
[\overline{\boldsymbol{\beta}}_{ij}]_{33} &= \frac{3}{2} i h_1 \cos\theta_{ij} \\
[\overline{\boldsymbol{\alpha}}_{ij}]_{11} &= [\overline{\boldsymbol{\alpha}}_{ij}]_{33} \\
[\overline{\boldsymbol{\alpha}}_{ij}]_{21} &= [\overline{\boldsymbol{\alpha}}_{ij}]_{12} e^{-i2\phi_{ij}} \\
[\overline{\boldsymbol{\alpha}}_{ij}]_{23} &= -[\overline{\boldsymbol{\alpha}}_{ij}]_{12} \\
[\overline{\boldsymbol{\alpha}}_{ij}]_{31} &= [\overline{\boldsymbol{\alpha}}_{ij}]_{13} e^{-i4\phi_{ij}} \\
[\overline{\boldsymbol{\alpha}}_{ij}]_{32} &= -[\overline{\boldsymbol{\alpha}}_{ij}]_{12} \\
[\overline{\boldsymbol{\beta}}_{ij}]_{11} &= -[\overline{\boldsymbol{\beta}}_{ij}]_{33} \\
[\overline{\boldsymbol{\beta}}_{ij}]_{21} &= [\overline{\boldsymbol{\beta}}_{ij}]_{12} e^{-i\phi_{ij}} \\
[\overline{\boldsymbol{\beta}}_{ij}]_{23} &= [\overline{\boldsymbol{\beta}}_{ij}]_{12} \\
[\overline{\boldsymbol{\beta}}_{ij}]_{32} &= [\overline{\boldsymbol{\beta}}_{ij}]_{21} \\
[\overline{\boldsymbol{\beta}}_{ij}]_{13} &= -[\overline{\boldsymbol{\beta}}_{ij}]_{22} = [\overline{\boldsymbol{\beta}}_{ij}]_{31} = 0.
\end{aligned} \tag{32}$$

In the above, h_0, h_1, and h_2 are the spherical Hankel functions with the appropriate arguments. With this explicit expression, it is easy to parallelize the matrix-fill part. One of the strength of CM-5 is on matrix operations. Hence, instead of using "do loops" in standard FORTRAN to compute r_{ij}, θ_{ij}, ϕ_{ij}, and $h_0(kr_{ij})$, etc., for each $i, j = 1, 2, \ldots, N$, we use the statement on the CM-5,

```
for all (i=1:n, j=1:n) r(i,j)=sqrt((x(i)-x(j))**2
                                   +(y(i)-y(j))**2
                                   +(z(i)-z(j))**2)
```

to compute r_{ij}, and similarly for θ_{ij} and ϕ_{ij}. Having obtained the above, we can compute the following efficiently by performing matrix operations. For example, the CM-5 FORTRAN code will appear as

```
h_0=exp(i*k_0*r)/(k_0*r)
h_1=h_0*(1/(k_0*r)-1)
h_2=3*h_1/(k_0*r)-h_0
beta(:,:,3,3)=1.5*i*cos(theta)*h_1
```

This paprallel implementation makes the matrix-fill part a small portion of total CPU time. A similar procedure is used to parallelize the computation of $\overline{\mathbf{h}}^{(i)}$ and $\overline{\mathbf{h}}^{(o)}$ matrices.

An estimated throughput of about 1 GFLOPS on a 64 processor partition of the CM-5 was obtained using this approach.

6. Numerical Results

Using this algorithm, we have developed a program to compute the scattering solution of a rectangular cubic dielectric scatterer. In our numerical simulation, 6 spherical modes (3 for TE and 3 for TM) are used to expand the scattered field of a subscatterer. Figures 4a and Figure 4b show the scattered field (magnitude and phase, respectively) of a cubic dielectric scatterer with side length $a = b = c = 1.6\lambda$ and $\epsilon_r = 2.6$. The incident wave is coming from $\theta = 180^0$ and $\phi = 0^0$ with θ polarization and a frequency of 300 MHz. The scattered field is observed at $\theta = 0^0$ to $\theta = 180^0$ and $\phi = 0^0$. Only the E_θ component is plotted. The results agree well with that of the brute-force solution using Gaussian elimination.

Figure 5 shows RCS of a dielectric rod of radius 0.4λ and of length 0.8λ, with $\epsilon_r = 2.05$. The discretization $\Delta = 0.1\lambda$, while the wave is incident from the axis of the cylinder, and the RCS is plotted as a function of the off-axis angle. The result compares well with the brute-force solution using Gaussian elimination.

As for the computational complexity, Figure 6 shows the comparison of the CPU time (on the CM-5) of this method (NEPAL) with the brute force solution. It is seen that when N, the number of unknowns, is small, NEPAL is not as efficient as brute force. However, when N is large, NEPAL becomes more efficient than brute force. The cross over occurs at about $N = 1800$. It is also seen that the slope of the CPU time curve for NEPAL is decreasing, and approaches the slope of an N^2 curve.

7. Conclusion

We have presented in this paper the extension of the nested equivalence principle algorithm (NEPAL) to three dimensions. The algorithm is based on Huygens' equivalence principle by nesting small algorithms within a larger one. Therefore, the key element is to divide the computation into several stages and reduce the number of unknowns at each stage. This represents an efficient algorithm for directly solving the integral equation of scattering with reduced computational complexity of $O(N^2)$. In other words, this method seeks the inverse of the integral operator in less than $O(N^3)$ operations. Hence, it can be used to compute the scattering solution of large objects for many incident waves.

REFERENCES

[1] W. C. Chew and C. C. Lu, "The use of Huygens' equivalence principle for solving the volume integral equation of scattering," *IEEE Trans. Antennas Propagat.*, vol. AP-41, no. 7, pp. 897-904, July 1993.

[2] Y. M. Wang and W. C. Chew, "A recursive T-matrix approach for the solution of electromagnetic scattering by many spheres," *IEEE Trans. Antennas Propagat.*, vol. AP-41, no. 12, pp. 1633-1639, December 1993.

[3] W. C. Chew, *Waves and Fields in Inhomogeneous Media*: Van Nostrand Reinhold, New York, 1990.

[4] J. D. Jackson, *Classical Electrodynamics* , Second Edition, John Wiley & Sons, New York, 1975.

[5] W. C. Chew and Y. M. Wang, " Efficient ways to compute the vector addition theorem," *J. Electromag. Waves and Appl.*, vol.7, no. 5, pp.651-665, 1993.

[6] W. C. Chew, J. Friedrich, and R. Geiger, "A multiple scattering solution for the effective permittivity of a sphere mixture," *IEEE Geoscience and Remote Sensing*, vol. 28, no. 2, p. 207, 1990.

[7] B. Peterson and S. Ström, "T-matrix for electromagnetic scattering from an arbitrary number of scatterers and representation of E(3)," *Phys. Rev.*, D8, pp. 3661-3678, 1973.

[8] C. Lanczos, *Applied Analysis*, p.41, Prentice-Hall, Englewood Cliffs, N. J. 1956.

[9] L. Gürel and W. C. Chew, "Recursive algorithms for calculating the scattering from N strips or patches," *IEEE Trans. Antennas Propagat.*, vol. AP-38, no. 4, pp. 507-515, April 1990.

[10] A. George, "Nested dissection of a regular finite element mesh," *SIAM J. Numer. Anal.*, vol. 10, pp. 345-363, 1973.

[11] J.H. Richmond, "Scattering by a dielectric cylinder of arbitrary cross section shape," *IEEE Trans. Antennas Propagat.*, vol. AP-14, no. 4, pp. 460-464, July 1966.

[12] G. P. Otto and W. C. Chew, "Inverse scattering of Hz waves using local shape function imaging: a T-matrix formulation," *Int. J. Imaging Sys. Tech.*, vol. 5, pp. 22-27, 1994.

[13] L. Tsang and C. E. Mandt, "Monte-carlo simulations of the extinction rate of dense media with randomly distributed dielectric spheres based on solution of Maxwell's equations," *Optics Letters*, vol. 17, No. 5, pp.

314-316, March 1, 1992.

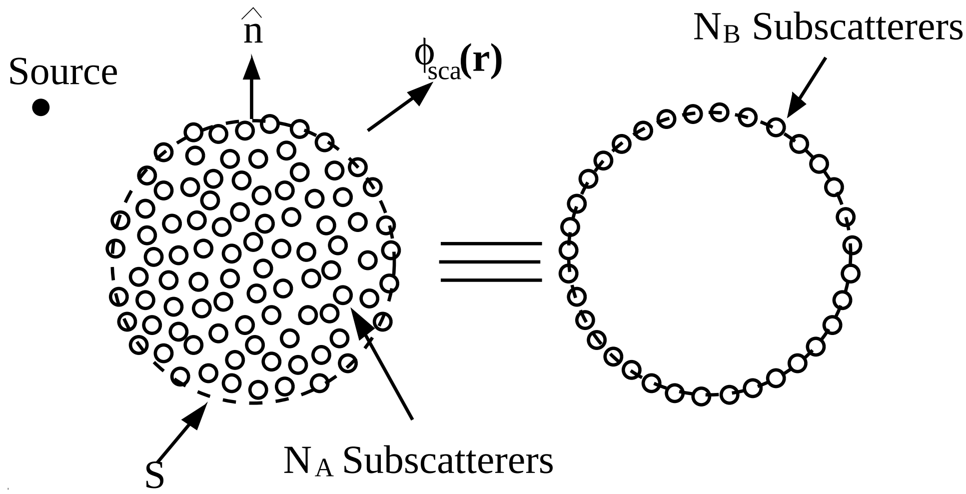

Figure 1. The replacement of volume scattering centers by surface scattering centers using Huygens' principle can greatly reduce the number of scattering centers needed to represent the scatterer.

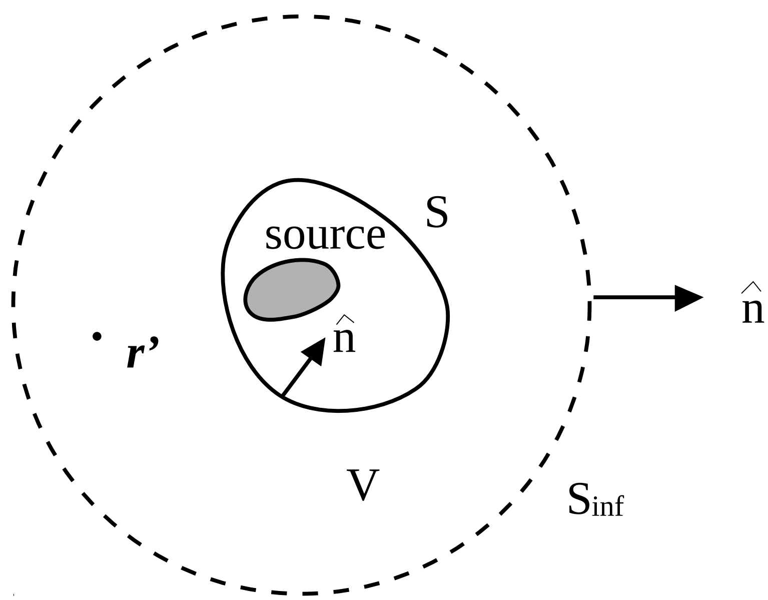

Figure 2. The Huygens' equivalence principle.

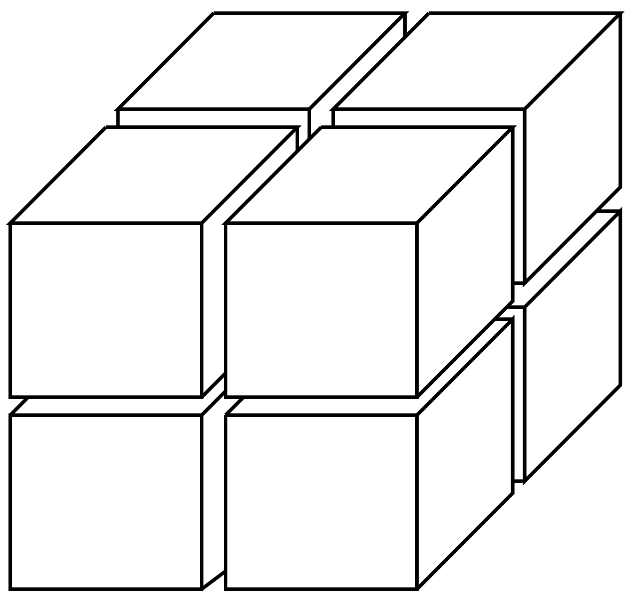

Figure 3. At the lowest level, each cubic box representing a group contains 64 subscatterers. The scattering solution of each group can be found, and then grouped by groups of two for the next level.

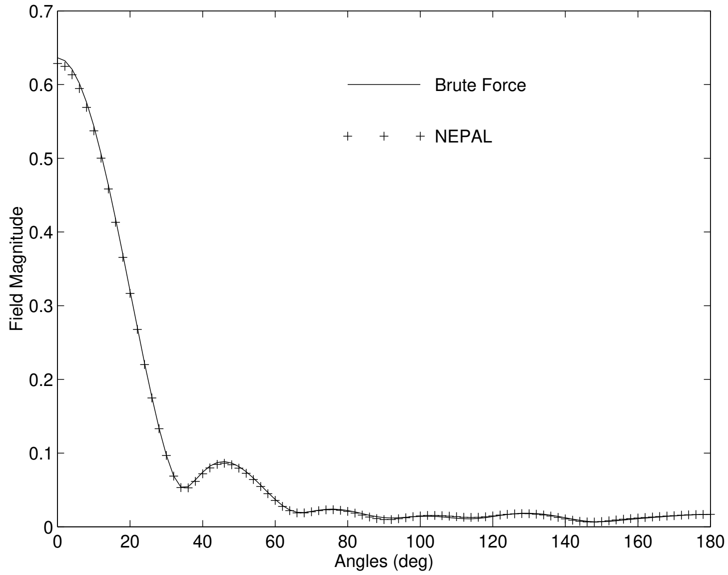

Figure 4. (a) Scattered field (magnitude) of a cubic dielectric scatterer for plane wave incidence at $\theta = 180^o$. Side length $= 1.6\lambda$, $\epsilon_r = 2.6$, $f = 300(MHz)$. Field points are on the circle of $r = 10\lambda$. The cube is divided into 512 small subscatterers.

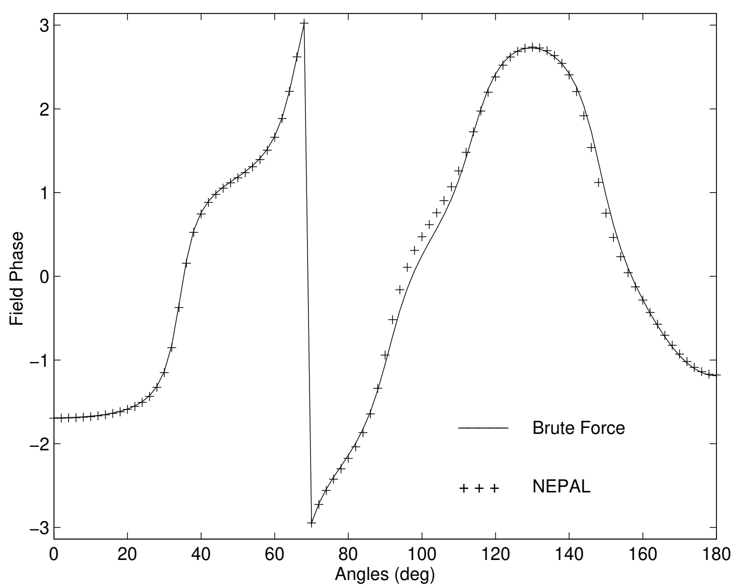

Figure 4. (b) Scattered field (phase) of a dielectric cube with the same parameters as in (a).

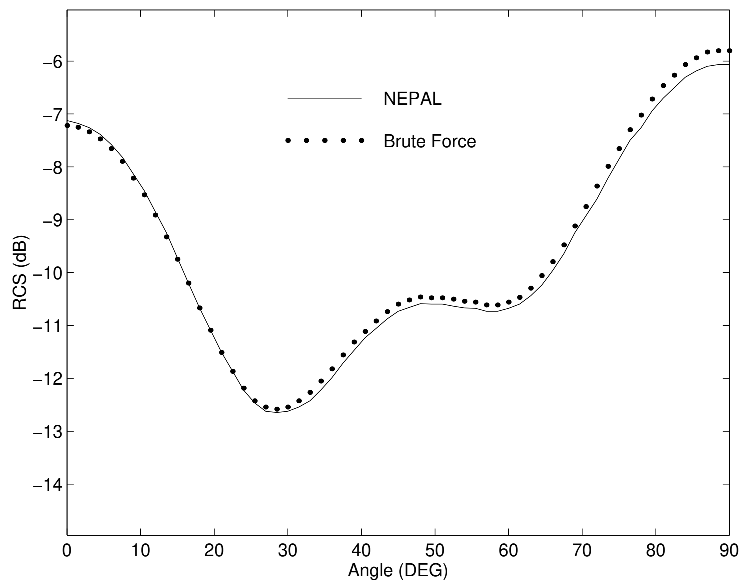

Figure 5. The RCS of a circular dielectric rod of finite length whose radius is 0.4λ, length is 0.8λ, and with $\epsilon_r = 2.05$. The discretization $\Delta = 0.1\lambda$, the incident wave is from the axis, and the RCS is plotted as a function of off-axis angle.

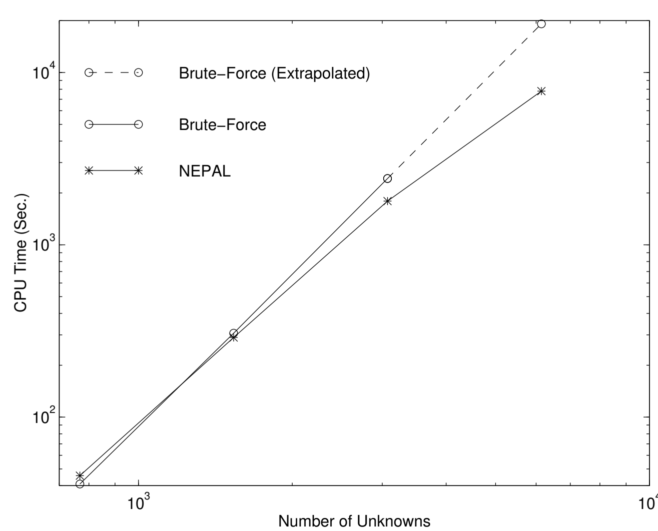

Figure 6. Comparison of CPU time of NEPAL and Gaussian elimination.